

Entangled multiplets and unusual spreading of quantum correlations in a continuously monitored tight-binding chain

Federico Carollo¹ and Vincenzo Alba²

¹*Institut für Theoretische Physik, Universität Tübingen,
Auf der Morgenstelle 14, 72076 Tübingen, Germany*

²*Dipartimento di Fisica, Università di Pisa, and INFN Sezione di Pisa, Largo Bruno Pontecorvo 3, Pisa, Italy*

We analyze the dynamics of entanglement in a paradigmatic noninteracting system subject to continuous monitoring of the local excitation densities. Recently, it was conjectured that the evolution of quantum correlations in such system is described by a semi-classical theory, based on entangled pairs of ballistically propagating quasiparticles and inspired by the hydrodynamic approach to unitary (integrable) quantum systems. Here, however, we show that this conjecture does not fully capture the complex behavior of quantum correlations emerging from the interplay between coherent dynamics and continuous monitoring. We unveil the existence of multipartite quantum correlations which are inconsistent with an entangled-pair structure and which, within a quasiparticle picture, would require the presence of larger multiplets. We also observe that quantum information is highly delocalized, as it is shared in a collective *nonredundant* way among adjacent regions of the many-body system. Our results shed new light onto the behavior of correlations in quantum stochastic dynamics and further show that these may be enhanced by a (weak) continuous monitoring process.

The evolution of quantum correlations in stochastic systems is attracting much attention nowadays [1–11]. On one hand, this dynamics is relevant for understanding the extent to which quantum effects may be exploited in current devices [12–20]. On the other, this renewed interest has been triggered by the discovery of entanglement phase transitions [21–43], stemming from the competition between coherent dynamics and random measurements. Furthermore, quantum stochastic processes hold the promise to bridge recent progress in the description of nonequilibrium unitary quantum systems and open challenges in characterizing open quantum dynamics [44–53], also beyond average-state properties [54–57]. In this regard, demonstrating the applicability of powerful theories, so-called quasiparticle pictures [58–61], to entanglement spreading in stochastic many-body processes would represent a major breakthrough.

This possibility has been explored in a paradigmatic many-body quantum system [62], subject to continuous monitoring [63] [see sketch in Fig. 1(a-b)]. It has been proposed that, as it happens for unitary (integrable) dynamics [58–61], the spreading of correlations in the system is solely attributable to entangled pairs of ballistically propagating quasiparticles [4]. The effect of continuous monitoring was conjectured to be that of making these excitations unstable and of generating new entangled pairs, in place of the collapsed ones [4]. This *collapsed quasiparticle ansatz* [4] has been benchmarked against exact numerics for the von Neumann entanglement entropy, showing remarkable results [4, 11].

In this paper, however, we demonstrate that continuously monitored systems feature an unexpectedly complex dynamics of quantum correlations, whose fundamental aspects are not captured by the collapsed quasiparticle ansatz. We show indeed that such a theory is not quantitatively accurate in predicting several measures of

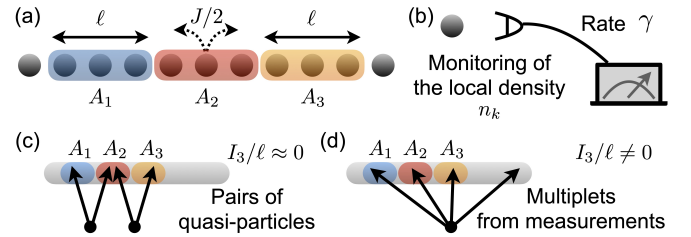


FIG. 1. Noninteracting system subject to continuous monitoring. a) Fermionic tight-binding chain with coherent hopping rate $J/2$. We consider several partitioning of this many-body system, $A \cup \bar{A}$, into a system of interest A and its complement, \bar{A} . In the sketch, we illustrate a system A made of three adjacent subsystems, $A = A_1 \cup A_2 \cup A_3$, of equal length ℓ . b) Each site of the chain is subject to the continuous measurement of its local density n_m , at rate γ . c) The tripartite mutual information I_3 quantifies the degree of extensivity of the mutual information and is also a fourpartite entanglement measure for pure states [64]. Pairs of quasiparticles cannot entangle more than two intervals at a same time, implying $I_3/\ell \rightarrow 0$. d) Multiplets with at least four quasiparticles can lead to a finite tripartite mutual information I_3/ℓ .

bipartite entanglement, both between a subsystem and the remainder of the many-body system and between adjacent subsystems. In this latter setting, we observe that continuous monitoring can also be, quite surprisingly, beneficial for quantum correlations, since it can stabilize a stationary entanglement in cases in which the unitary dynamics would lead to unentangled subsystems.

Most importantly, we identify a central reason why the dynamics of quantum correlations in the system cannot be captured by a picture based on quasiparticle pairs. We compute the *tripartite mutual information* between three subsystems A_1, A_2, A_3 [see sketch in Fig. 1(a)] and show that it assumes nonzero, in fact negative, values. This signals the existence of multipartite (i.e., between

more than two intervals) quantum correlations, which are inconsistent with the mere presence of pairs of entangled quasiparticles [cf. Fig. 1(c)]. As we discuss, consistency of a quasiparticle picture with a nonzero tripartite mutual information requires the presence of entangled multiplets with at least four quasiparticles, as sketched in Fig. 1(d).

A negative tripartite mutual information, as we find here, implies that the information about A_2 contained in $A_1 \cup A_3$ is more than the sum of the information contained in A_1 and A_3 separately [65], showing that for the monitored system *the whole is more than the sum of its parts* [66]. It further indicates that the mutual information is monogamous and, thus, likely to be dominated by quantum correlations [66–70]. Negative values of the tripartite mutual information have also been associated with the delocalization (broadly referred to as *scrambling*) of quantum information [64–66, 70–76]. Our findings show that the interplay between monitoring and coherent dynamics leads to the continuous dispersal of quantum information into entangled multiplets of excitations, which in turn establish robust multipartite entanglement and determine an unusual, for a noninteracting system, dynamics of quantum correlations.

Monitored noninteracting system.— We consider a fermionic chain subject to the continuous measurement of local observables [4, 8]. The model Hamiltonian is

$$H = \frac{J}{2} \sum_{m=1}^L \left(a_m^\dagger a_{m+1} + a_{m+1}^\dagger a_m \right), \quad (1)$$

with a_m, a_m^\dagger being fermionic annihilation and creation operators. This Hamiltonian describes coherent hopping of fermionic excitations between neighboring sites at rate $J/2$ [cf. Fig. 1(a)], in a periodic lattice. The total number of fermionic excitations $N = \sum_{m=1}^L n_m$, with $n_m = a_m^\dagger a_m$, is conserved and we assume that the local fermionic densities n_m are continuously measured, as sketched in Fig. 1(b). This monitoring induces non-linear and random effects in the system dynamics, which is governed by the stochastic Schrödinger equation [63, 77–79]

$$d|\psi(t)\rangle = -iHdt|\psi(t)\rangle + \sum_{m=1}^L \left(\sqrt{\gamma} M_m(t) dW_m(t) - \frac{\gamma}{2} M_m^2(t) dt \right) |\psi(t)\rangle, \quad (2)$$

where $M_m(t) = n_m - \langle \psi(t) | n_m | \psi(t) \rangle$. The terms $dW_m(t)$ are Wiener processes — in Ito convention — such that $\mathbb{E}[dW_m(t)] = 0$ and $\mathbb{E}[dW_m(t)dW_{m'}(t)] = \delta_{mm'} dt$, with \mathbb{E} denoting expectation over noise realizations. The rate γ provides the strength of the monitoring process.

We consider the initial state to be the Néel state $|\psi(0)\rangle = \prod_{m \text{ odd}} a_m^\dagger |0\rangle$, where $|0\rangle$ is the fermionic vacuum. For each noise realization, Eq. (2) encodes a quantum trajectory. Since the initial state is Gaussian

and the generator is quadratic, the state in each trajectory is Gaussian at all times and can be efficiently simulated [4, 8]. In particular, entanglement-related quantities, such as the Rényi entropies $S_\ell^{(n)}(t)$ of a subsystem of length ℓ , in quantum trajectories can be calculated from the fermionic two-point function $C_{hk} = \langle \psi(t) | a_h^\dagger a_k | \psi(t) \rangle$ [80]. In what follows, we focus on the behavior of the entropies $\bar{S}_\ell^{(n)}(t) := \mathbb{E}[S_\ell^{(n)}(t)]$, and related quantities, averaged over quantum trajectories.

Collapsed quasiparticle ansatz.— In the absence of continuous monitoring ($\gamma \equiv 0$), the unitary dynamics of quantum information in the system is captured by a quasiparticle picture [58–61]. The basic idea is that the initial state of the system acts as a source of pairs of entangled quasiparticles, labelled by their quasi-momentum q , which travel ballistically in opposite direction with velocity $|v_q| = |J \sin(q)|$. While travelling, quasiparticles spread correlations along the system. Specifically, the entanglement between a subsystem and its complement, at a given time, is proportional to the number of quasiparticle pairs they share at that time. For instance, the Rényi- n entanglement entropy of a subsystem of length ℓ , embedded in an infinite chain, is given by [59]

$$S_\ell^{(n),0}(t) = \int_{-\pi}^{\pi} \frac{dq}{2\pi} s_q^{(n)} \Theta_q(t). \quad (3)$$

This equation is valid in the scaling limit $t, \ell \rightarrow \infty$, with $t/\ell = \tau$ fixed, and provides the leading-order behavior in ℓ . The superscript 0 stands for unitary dynamics and

$$\Theta_q(t) = \min\{2|v_q|t, \ell\}. \quad (4)$$

This function counts the number of pairs, formed by quasiparticles with quasimomenta q and $-q$, shared by the subsystem and its complement at time t [58]. The term $s_q^{(n)}$ accounts for the entanglement between such quasiparticles and is given by the Yang-Yang entropy

$$s_q^{(n)} = (1-n)^{-1} \log [\varrho_q^n + (1-\varrho_q)^n], \quad (5)$$

quantifying the quasimomentum contribution to the thermodynamic entropy of the generalized Gibbs ensemble describing local stationary properties of the system [81–86]. In Eq. (5), ϱ_q is the density of quasiparticles $\varrho_q = \langle \psi(0) | \beta_q^\dagger \beta_q | \psi(0) \rangle$ and β_q are the eigenmodes of the Hamiltonian H . For the Néel state, $\varrho_q = 1/2, \forall q$.

To account for the presence of continuous monitoring, a modification to the above picture, also called collapsed quasiparticle ansatz, has been proposed [4]. The key assumptions are that quantum correlations are still exclusively spread by pairs of quasiparticles and that the measurement process solely determines their random collapse, at a rate proportional to γ . When such an event occurs, the collapsed pair becomes irrelevant. However, in its place, a new entangled pair is produced, uniformly

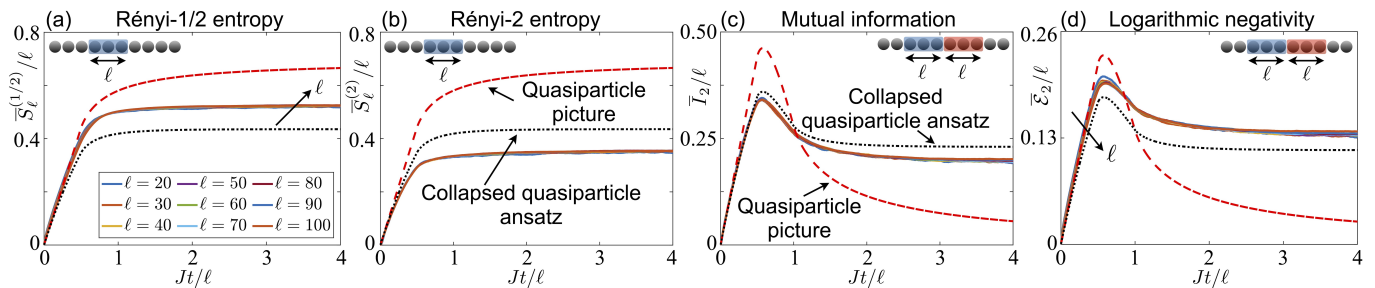


FIG. 2. **Entanglement and quantum correlations in the monitored system.** a) Average Rényi-1/2 entropy for a subsystem of length ℓ — see sketch — quantifying entanglement between the subsystem and its complement (the remainder of the system). The dashed line is the unitary prediction from Eq. (3), while the dotted line is the one from Eq. (6). Solid lines are numerical results. We have taken $\Gamma/J = 1$. (b) Same as in (a) but for the Rényi-2 entanglement entropy. The predictions coincide with the ones in (a), see main text. (c) Mutual information \bar{I}_2 [cf. Eq. (7)] between two adjacent subsystems of length ℓ , as shown in the sketch. Also in this case, the dashed line is the prediction for the unitary case $\gamma \equiv 0$, while the dotted one is the prediction from the collapsed quasiparticle ansatz (see Ref. [87]). (d) Logarithmic negativity $\bar{\mathcal{E}}_2$ quantifying entanglement between two adjacent subsystems. Both predictions coincide with half of those obtained for the mutual information [87]. For all panels, we considered $L = 1000$. In (a-b), we averaged over $N_{\text{traj}} = 250$ trajectories, in (c) $N_{\text{traj}} = 150$ while in (d) $N_{\text{traj}} = 100$.

in quasimomentum. For (macroscopically) homogeneous initial states, such as the Néel state, it was assumed that the entanglement content of any pair, either generated in the initial state or during the dynamics, is a function of the average density [4], which is conserved by Eq. (2).

From this stochastic picture, one can make predictions for the Rényi entropy of a subsystem averaged over trajectories. For homogeneous initial states, one has [4]

$$\bar{S}_\ell^{(n)}(t) = e^{-\gamma t} S_\ell^{(n),0}(t) + \gamma \int_0^t du e^{-\gamma u} S_\ell^{(n),0}(u). \quad (6)$$

As for the unitary case, this equation is expected to provide the leading-order behavior in the scaling limit $t, \ell \rightarrow \infty$, with $\tau = t/\ell$ fixed. Since we have $t \propto \ell$, to make Eq. (6) well-defined in the $\ell \rightarrow \infty$ limit, it is natural to consider a small γ , obtained through the rescaling $\gamma = \Gamma/\ell$, such that $\gamma t = \Gamma\tau$ remains fixed in the limit [4, 44, 48–51] (see Supplemental Material [87]). The first term in Eq. (6) accounts for correlations due to quasiparticle pairs formed in the initial state and survived up to time t . The second term instead accounts for pairs generated after the random collapses [4]. For $\gamma \equiv 0$, one recovers the unitary case $\bar{S}_\ell^{(n)}(t) = S_\ell^{(n),0}(t)$. Since $s_q^{(n)} = \log 2 \forall n$, Eqs. (3)-(6) give the same quantitative prediction for all Rényi entropies.

Entanglement and quantum correlations.— We first analyze entanglement between a subsystem of length ℓ and its complement (the remainder of the many-body system), as sketched in Fig. 2(a). We consider the Rényi-1/2 entanglement entropy of the subsystem, which for each quantum trajectory is *exactly* equal to the logarithmic negativity [88–95], since the system state is pure [96]. As shown in Fig. 2(a), numerical results for $\bar{S}_\ell^{(1/2)}$ do not agree with the prediction from Eq. (6) (dotted line).

This also happens for the Rényi entropy with $n = 2$ [see Fig. 2(b)]. As reported in Ref. [87], we even observe discrepancies between numerical results and the prediction for the von Neumann entropy analyzed in Ref. [4], when systematically considering the scaling limit. In Fig. 2 (a-b), we also show the theory prediction for $\gamma \equiv 0$ (dashed line) given by Eq. (3). In the scaling limit $\bar{S}_\ell^{(n)}$ and $S_\ell^{(n),0}$ are of the same order, even if the monitoring process suppresses here quantum correlations.

We now consider bipartite correlations between two subsystems embedded in the chain. We start investigating the von Neumann mutual information, defined as

$$I_2[X, Y] := S^{(n \rightarrow 1)}[X] + S^{(n \rightarrow 1)}[Y] - S^{(n \rightarrow 1)}[X \cup Y], \quad (7)$$

where $S^{(n \rightarrow 1)}[X]$ indicates the von Neumann entropy of the system X . In particular, we take two adjacent subsystems, A_1 and A_2 , of length ℓ [see sketch in Fig. 2(c)]. Within the collapsed quasiparticle ansatz, the prediction for the average mutual information — which we derived in Ref. [87] — is given by an equation similar to Eq. (6), with unitary term given by Eq. (3) with $\Theta_q(t) = 2|v_q|t + 2 \max\{|v_q|t, \ell\} - 2 \max\{2|v_q|t, \ell\}$ [87]. This function $\Theta_q(t)$ now counts the number of quasiparticle pairs shared by the intervals A_1 and A_2 [97].

As shown in Fig. 2(c), $\bar{I}_2(t)$ exhibits clear scaling behavior in the limit. Still, as for the entanglement entropies, the theoretical prediction fails to capture quantitatively the mutual information. For instance, our results show that correlations between A_1 and A_2 do not decay to zero in the limit $t/\ell \rightarrow \infty$, in contrast with the unitary case (dashed line), but reach a plateau value. While this feature is qualitatively captured by the ansatz [87], the exact stationary value is substantially different. The existence of this plateau demonstrates that the continuous monitoring enhances bipartite correlations. This is due to the fact that the monitoring generates,

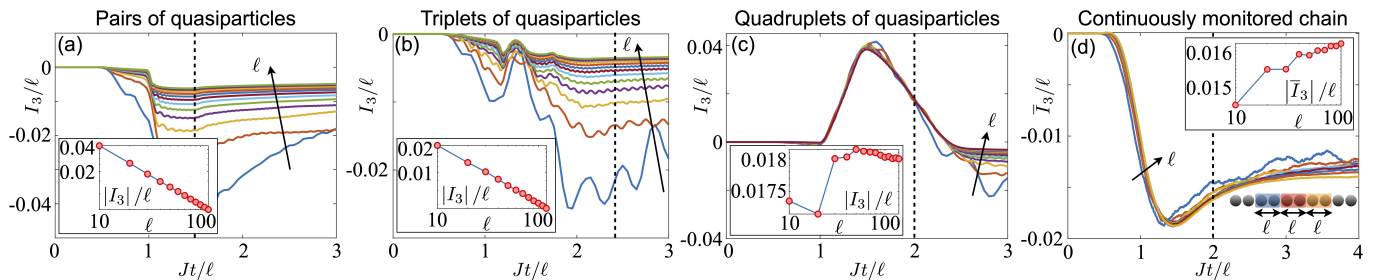


FIG. 3. **Tripartite mutual information.** a) Dynamics of the tripartite mutual information starting from the Néel state, for $\gamma \equiv 0$. In the scaling limit $\ell \rightarrow \infty$, this quantity is subextensive in ℓ . The inset (in log-log scale) shows convergence to zero of $|I_3|/\ell$, for $Jt/\ell = 1.5$. We considered $\ell = 10, 20, \dots, 120$ and L up to $L = 1200$. b) Tripartite mutual information starting from a state with one fermionic excitation every three sites, for $\gamma \equiv 0$. A subextensive behavior with ℓ of this quantity is apparent. The inset (in log-log scale) shows $|I_3|/\ell$ as a function of ℓ , for $Jt/\ell = 2.4$. We considered $\ell = 10, 20, \dots, 120$ and L up to $L = 1200$. c) Tripartite mutual information starting from a state with one fermionic excitation every four sites, for $\gamma \equiv 0$. This quantity is extensive in ℓ and remains finite in the scaling limit, as also highlighted in the inset (in log-log scale) for $Jt/\ell = 2$. We considered $\ell = 10, 20, \dots, 140$ and L up to $L = 1500$. d) Average tripartite mutual information, \bar{I}_3 , for the continuously monitored system sketched in Fig. 1(a-b), with $\Gamma/J = 1$. As shown in the main panel, as well as in the inset (in log-log scale) for $Jt/\ell = 2$, the tripartite mutual information remains finite (negative) in the scaling limit $\ell \rightarrow \infty$. We considered $\ell = 10, 20, \dots, 100$ and L up to $L = 1000$. The value of \bar{I}_3 is obtained by averaging over $N_{\text{traj}} = 250$ quantum trajectories.

continuously in time, entangled excitations throughout the system, and their spreading sustains finite stationary correlations between the two subsystems. Since the quantum state of $A_1 \cup A_2$ is mixed, these correlations are in principle both of quantum and of classical nature. However, we can also calculate the logarithmic negativity $\bar{\mathcal{E}}_2(t)$ [88–95], a proper measure of entanglement, which shows that A_1 and A_2 are not solely classically correlated but feature a stationary entanglement, as shown in Fig. 2(d). The prediction from the collapsed quasiparticle ansatz for the logarithmic negativity is given by $\bar{\mathcal{E}}_2(t) = \bar{I}_2(t)/2$ [87]. This is due to the fact that for the unitary system the logarithmic negativity is equivalent to the Rényi-1/2 mutual information in the scaling limit [98], and that for our case the latter is equal to $I_2(t)$. The above prediction fails to capture the behavior of $\bar{\mathcal{E}}_2(t)$, as shown in Fig. 2(d).

Beyond quasiparticle pairs.— We now consider the tripartite mutual information I_3 between three adjacent intervals A_1, A_2, A_3 [cf. Fig. 1(a)],

$$I_3 := I_2[A_2, A_1] + I_2[A_2, A_3] - I_2[A_2, A_1 \cup A_3]. \quad (8)$$

This quantity allows us to discuss multipartite correlations — I_3 is a fourpartite entanglement measure for pure states — and to unveil peculiar features in the behavior of quantum correlations in the system.

By definition, the tripartite mutual information is zero if the mutual information between A_2 and $A_1 \cup A_3$ is equal to the sum of the mutual information between A_2 and A_1 plus that between A_2 and A_3 . This simple property allows us to argue that the mere presence of quasiparticle pairs must result in a vanishing tripartite mutual information. Indeed, pairs of quasiparticles can entangle only two subsystems at a time and different entangling pairs

are uncorrelated with each other. This implies that the contributions of the pairs that entangle A_2 with A_1 and A_3 are subtracted by the last term in Eq. (8), so that $I_3 = 0$ in the scaling limit. In Fig. 3(a), as an example, we show how I_3 vanishes for the unitary dynamics implemented by H , when starting from the Néel state.

Furthermore, in Ref. [87] we demonstrate that not even triplets of quasiparticles can produce a finite tripartite mutual information, in the scaling limit. We also verified this numerically [see Fig. 3(b)] for the unitary dynamics implemented by H starting from $|\psi(0)\rangle = \prod_k a_{3k+1}^\dagger |0\rangle$, which is a source of quasiparticle triplets [99]. On the other hand, multiplets with at least four elements can generate fourpartite entanglement [see sketch in Fig. 1(d)] giving rise to a nonvanishing I_3/ℓ , in the $\ell \rightarrow \infty$ limit. This is shown in Fig. 3(c), obtained unitarily evolving the initial state $|\psi(0)\rangle = \prod_k a_{4k+1}^\dagger |0\rangle$, which is a source of quadruplets of quasiparticles [99].

We can thus exploit the tripartite mutual information to witness the existence of multiplets with at least four excitations in the process of Eq. (2). As shown in Fig. 3(d), the average tripartite mutual information \bar{I}_3 is indeed different from zero. In particular, it assumes negative values, in contrast to the unitary dynamics shown in Fig. 3(c). We also observed that, for unitary dynamics, I_3 remains positive also in the presence of larger multiplets. This suggests that, in the Hamiltonian case, quantum information is shared in a redundant way among the different quasiparticles, i.e., they all share the same piece of information. On the other hand, in the presence of continuous monitoring we find $\bar{I}_3 < 0$, which indicates that the mutual information is monogamous [66–70], $I_2[A_2, A_1 \cup A_3] > I_2[A_2, A_1] + I_2[A_2, A_3]$, and implies that there is more information about A_2 in $A_1 \cup A_3$ than in the sum of A_1 and A_3 , separately. For

the stochastic process, quantum information is thus highly delocalized, i.e., continuously and collectively distributed into the different excitations generated by the monitoring process and dispersed throughout the system by the coherent dynamics.

Conclusions.— We have shown that the dynamics of quantum correlations in a paradigmatic continuously monitored system is unexpectedly complex and displays interesting unanticipated features. Such intricate phenomenology cannot be explained solely relying on entangled pairs of quasiparticles, and we have indeed provided evidence for the existence of multiplets of excitations with at least four elements. From a fundamental perspective our results suggest that, if a quasiparticle picture for the process in Eq. (2) exists, it cannot be solely based on an entangled-pair structure. We have further found that quantum correlations, including entanglement, can be enhanced by continuous monitoring [cf. Fig. 2(c-d)]. The latter is also responsible for a robust delocalization of quantum information, which is shared by different subsystems in a genuinely collective way.

Finally, we note that quantum correlations in the average state, $\rho(t) = \mathbb{E} [|\psi(t)\rangle\langle\psi(t)|]$, of noninteracting Lindblad dynamics are, in general, fully captured by a picture based on pairs of quasiparticles [47, 49–51].

Acknowledgements.— F.C. acknowledges support from the “Wissenschaftler-Rückkehrprogramm GSO/CZS” of the Carl-Zeiss-Stiftung and the German Scholars Organization e.V., as well as through the Deutsche Forschungsgemeinschaft (DFG, German Research Foundation) under Project No. 435696605, as well as through the Research Unit FOR 5413/1, Grant No. 465199066. F.C. is indebted to the Baden-Württemberg Stiftung for the financial support by the Eliteprogramme for Postdocs.

-
- [1] A. Nahum, J. Ruhman, S. Vijay, and J. Haah, Quantum Entanglement Growth under Random Unitary Dynamics, *Phys. Rev. X* **7**, 031016 (2017).
- [2] A. Nahum, S. Vijay, and J. Haah, Operator Spreading in Random Unitary Circuits, *Phys. Rev. X* **8**, 021014 (2018).
- [3] T. Zhou and A. Nahum, Emergent statistical mechanics of entanglement in random unitary circuits, *Phys. Rev. B* **99**, 174205 (2019).
- [4] X. Cao, A. Tilloy, and A. D. Luca, Entanglement in a fermion chain under continuous monitoring, *SciPost Phys.* **7**, 24 (2019).
- [5] M. Žnidarič, Entanglement growth in diffusive systems, *Communications Physics* **3**, 100 (2020).
- [6] L. Piroli, C. Sünderhauf, and X.-L. Qi, A random unitary circuit model for black hole evaporation, *Journal of High Energy Physics* **2020**, 63 (2020).
- [7] A. Nahum, S. Roy, B. Skinner, and J. Ruhman, Measurement and Entanglement Phase Transitions in All-To-All Quantum Circuits, on Quantum Trees, and in Landau-Ginsburg Theory, *PRX Quantum* **2**, 010352 (2021).
- [8] O. Alberton, M. Buchhold, and S. Diehl, Entanglement Transition in a Monitored Free-Fermion Chain: From Extended Criticality to Area Law, *Phys. Rev. Lett.* **126**, 170602 (2021).
- [9] A. Lavasani, Y. Alavirad, and M. Barkeshli, Measurement-induced topological entanglement transitions in symmetric random quantum circuits, *Nature Physics* **17**, 342 (2021).
- [10] M. Ippoliti, M. J. Gullans, S. Gopalakrishnan, D. A. Huse, and V. Khemani, Entanglement Phase Transitions in Measurement-Only Dynamics, *Phys. Rev. X* **11**, 011030 (2021).
- [11] M. Coppola, E. Tirrito, D. Karevski, and M. Collura, Growth of entanglement entropy under local projective measurements, *arXiv:2109.10837* (2021).
- [12] A. Peruzzo, J. McClean, P. Shadbolt, M.-H. Yung, X.-Q. Zhou, P. J. Love, A. Aspuru-Guzik, and J. L. O’Brien, A variational eigenvalue solver on a photonic quantum processor, *Nature Communications* **5**, 4213 (2014).
- [13] J. Preskill, Quantum Computing in the NISQ era and beyond, *Quantum* **2**, 79 (2018).
- [14] A. Kandala, K. Temme, A. D. Córcoles, A. Mezzacapo, J. M. Chow, and J. M. Gambetta, Error mitigation extends the computational reach of a noisy quantum processor, *Nature* **567**, 491 (2019).
- [15] V. Havlíček, A. D. Córcoles, K. Temme, A. W. Harrow, A. Kandala, J. M. Chow, and J. M. Gambetta, Supervised learning with quantum-enhanced feature spaces, *Nature* **567**, 209 (2019).
- [16] G. G. Guerreschi and A. Y. Matsuura, QAOA for Max-Cut requires hundreds of qubits for quantum speed-up, *Scientific Reports* **9**, 6903 (2019).
- [17] F. Arute, K. Arya, R. Babbush, D. Bacon, and J. C. Bardin et al., Quantum supremacy using a programmable superconducting processor, *Nature* **574**, 505 (2019).
- [18] H.-S. Zhong, H. Wang, Y.-H. Deng, M.-C. Chen, L.-C. Peng, Y.-H. Luo, J. Qin, D. Wu, X. Ding, Y. Hu, P. Hu, X.-Y. Yang, W.-J. Zhang, H. Li, Y. Li, X. Jiang, L. Gan, G. Yang, L. You, Z. Wang, L. Li, N.-L. Liu, C.-Y. Lu, and J.-W. Pan, Quantum computational advantage using photons, *Science* **370**, 1460 (2020).
- [19] Y. Xia, W. Li, Q. Zhuang, and Z. Zhang, Quantum-Enhanced Sensor Data Classification with a Variational Entangled Sensor Network, *Phys. Rev. X* **11**, 021047 (2021).
- [20] K. Bharti, A. Cervera-Lierta, T. H. Kyaw, T. Haug, S. Alperin-Lea, A. Anand, M. Degroote, H. Heimonen, J. S. Kottmann, T. Menke, W.-K. Mok, S. Sim, L.-C. Kwек, and A. Aspuru-Guzik, Noisy intermediate-scale quantum algorithms, *Rev. Mod. Phys.* **94**, 015004 (2022).
- [21] Y. Li, X. Chen, and M. P. A. Fisher, Quantum Zeno effect and the many-body entanglement transition, *Phys. Rev. B* **98**, 205136 (2018).
- [22] B. Skinner, J. Ruhman, and A. Nahum, Measurement-Induced Phase Transitions in the Dynamics of Entanglement, *Phys. Rev. X* **9**, 031009 (2019).
- [23] A. Chan, R. M. Nandkishore, M. Pretko, and G. Smith, Unitary-projective entanglement dynamics, *Phys. Rev. B* **99**, 224307 (2019).
- [24] C.-M. Jian, Y.-Z. You, R. Vasseur, and A. W. W. Ludwig, Measurement-induced criticality in random quantum cir-

- uits, *Phys. Rev. B* **101**, 104302 (2020).
- [25] M. J. Gullans and D. A. Huse, Dynamical Purification Phase Transition Induced by Quantum Measurements, *Phys. Rev. X* **10**, 041020 (2020).
- [26] Y. Bao, S. Choi, and E. Altman, Theory of the phase transition in random unitary circuits with measurements, *Phys. Rev. B* **101**, 104301 (2020).
- [27] N. Lang and H. P. Büchler, Entanglement transition in the projective transverse field Ising model, *Phys. Rev. B* **102**, 094204 (2020).
- [28] D. Rossini and E. Vicari, Measurement-induced dynamics of many-body systems at quantum criticality, *Phys. Rev. B* **102**, 035119 (2020).
- [29] Q. Tang and W. Zhu, Measurement-induced phase transition: A case study in the nonintegrable model by density-matrix renormalization group calculations, *Phys. Rev. Research* **2**, 013022 (2020).
- [30] O. Lunt and A. Pal, Measurement-induced entanglement transitions in many-body localized systems, *Phys. Rev. Research* **2**, 043072 (2020).
- [31] A. Zabalo, M. J. Gullans, J. H. Wilson, S. Gopalakrishnan, D. A. Huse, and J. H. Pixley, Critical properties of the measurement-induced transition in random quantum circuits, *Phys. Rev. B* **101**, 060301 (2020).
- [32] O. Lunt, M. Szyniszewski, and A. Pal, Measurement-induced criticality and entanglement clusters: A study of one-dimensional and two-dimensional Clifford circuits, *Phys. Rev. B* **104**, 155111 (2021).
- [33] X. Turkeshi, A. Biella, R. Fazio, M. Dalmonte, and M. Schiró, Measurement-induced entanglement transitions in the quantum Ising chain: From infinite to zero clicks, *Phys. Rev. B* **103**, 224210 (2021).
- [34] M. Buchhold, Y. Minoguchi, A. Altland, and S. Diehl, Effective Theory for the Measurement-Induced Phase Transition of Dirac Fermions, *Phys. Rev. X* **11**, 041004 (2021).
- [35] S. Sang, Y. Li, T. Zhou, X. Chen, T. H. Hsieh, and M. P. Fisher, Entanglement Negativity at Measurement-Induced Criticality, *PRX Quantum* **2**, 030313 (2021).
- [36] T.-C. Lu and T. Grover, Spacetime duality between localization transitions and measurement-induced transitions, *PRX Quantum* **2**, 040319 (2021).
- [37] S.-K. Jian, C. Liu, X. Chen, B. Swingle, and P. Zhang, Measurement-Induced Phase Transition in the Monitored Sachdev-Ye-Kitaev Model, *Phys. Rev. Lett.* **127**, 140601 (2021).
- [38] U. Agrawal, A. Zabalo, K. Chen, J. H. Wilson, A. C. Potter, J. H. Pixley, S. Gopalakrishnan, and R. Vasseur, Entanglement and charge-sharpening transitions in $U(1)$ symmetric monitored quantum circuits, arXiv:2107.10279 (2021).
- [39] M. Block, Y. Bao, S. Choi, E. Altman, and N. Y. Yao, Measurement-Induced Transition in Long-Range Interacting Quantum Circuits, *Phys. Rev. Lett.* **128**, 010604 (2022).
- [40] T. Minato, K. Sugimoto, T. Kuwahara, and K. Saito, Fate of Measurement-Induced Phase Transition in Long-Range Interactions, *Phys. Rev. Lett.* **128**, 010603 (2022).
- [41] T. Müller, S. Diehl, and M. Buchhold, Measurement-Induced Dark State Phase Transitions in Long-Ranged Fermion Systems, *Phys. Rev. Lett.* **128**, 010605 (2022).
- [42] Y. Minoguchi, P. Rabl, and M. Buchhold, Continuous Gaussian Measurements of the Free Boson CFT: A model for Exactly Solvable and Detectable Measurement-Induced Dynamics, *SciPost Phys.* **12**, 9 (2022).
- [43] A. Zabalo, M. J. Gullans, J. H. Wilson, R. Vasseur, A. W. W. Ludwig, S. Gopalakrishnan, D. A. Huse, and J. H. Pixley, Operator Scaling Dimensions and Multifractality at Measurement-Induced Transitions, *Phys. Rev. Lett.* **128**, 050602 (2022).
- [44] F. Lange, Z. Lenarčič, and A. Rosch, Time-dependent generalized Gibbs ensembles in open quantum systems, *Phys. Rev. B* **97**, 165138 (2018).
- [45] D. Rossini and E. Vicari, Coherent and dissipative dynamics at quantum phase transitions, arXiv:2103.02626 (2021).
- [46] D. Rossini, A. Ghermaoui, M. B. Aguilera, R. Vatré, R. Bouganne, J. Beugnon, F. Gerbier, and L. Mazza, Strong correlations in lossy one-dimensional quantum gases: From the quantum Zeno effect to the generalized Gibbs ensemble, *Phys. Rev. A* **103**, L060201 (2021).
- [47] S. Maity, S. Bandyopadhyay, S. Bhattacharjee, and A. Dutta, Growth of mutual information in a quenched one-dimensional open quantum many-body system, *Phys. Rev. B* **101**, 180301 (2020).
- [48] I. Bouchoule, B. Doyon, and J. Dubail, The effect of atom losses on the distribution of rapidities in the one-dimensional Bose gas, *SciPost Phys.* **9**, 44 (2020).
- [49] V. Alba and F. Carollo, Spreading of correlations in Markovian open quantum systems, *Phys. Rev. B* **103**, L020302 (2021).
- [50] V. Alba and F. Carollo, Hydrodynamics of quantum entropies in Ising chains with linear dissipation, arXiv:2109.01836 (2021).
- [51] F. Carollo and V. Alba, Dissipative quasiparticle picture for quadratic Markovian open quantum systems, *Phys. Rev. B* **105**, 144305 (2022).
- [52] V. Alba, B. Bertini, M. Fagotti, L. Piroli, and P. Ruggiero, Generalized-Hydrodynamic approach to Inhomogeneous Quenches: Correlations, Entanglement and Quantum Effects, arXiv:2104.00656 (2021).
- [53] E. Starchl and L. M. Sieberer, Relaxation to a parity-time symmetric generalized Gibbs ensemble after a quantum quench in a driven-dissipative Kitaev chain, arXiv:220314589 (2022).
- [54] F. Carollo, R. L. Jack, and J. P. Garrahan, Unraveling the Large Deviation Statistics of Markovian Open Quantum Systems, *Phys. Rev. Lett.* **122**, 130605 (2019).
- [55] F. Carollo and C. Pérez-Espigares, Entanglement statistics in Markovian open quantum systems: A matter of mutation and selection, *Phys. Rev. E* **102**, 030104 (2020).
- [56] D. Bernard and L. Piroli, Entanglement distribution in the Quantum Symmetric Simple Exclusion Process, arXiv:2102.04745 (2021).
- [57] X. Turkeshi, L. Piroli, and M. Schiró, Enhanced entanglement negativity in boundary driven monitored fermionic chains, arXiv:2205.07992 (2022).
- [58] P. Calabrese and J. Cardy, Evolution of entanglement entropy in one-dimensional systems, *Journal of Statistical Mechanics: Theory and Experiment* **2005**, P04010 (2005).
- [59] M. Fagotti and P. Calabrese, Evolution of entanglement entropy following a quantum quench: Analytic results for the XY chain in a transverse magnetic field, *Phys. Rev. A* **78**, 010306 (2008).
- [60] V. Alba and P. Calabrese, Entanglement and thermodynamics after a quantum quench in integrable systems, *Proceedings of the National Academy of Sciences* **114**, 7947 (2017).

- [61] P. Calabrese, Entanglement and thermodynamics in non-equilibrium isolated quantum systems, *Physica A: Statistical Mechanics and its Applications* **504**, 31 (2018), lecture Notes of the 14th International Summer School on Fundamental Problems in Statistical Physics.
- [62] E. Lieb, T. Schultz, and D. Mattis, Two soluble models of an antiferromagnetic chain, *Annals of Physics* **16**, 407 (1961).
- [63] H. M. Wiseman and G. J. Milburn, *Quantum Measurement and Control* (Cambridge University Press, 2009).
- [64] P. Hosur, X.-L. Qi, D. A. Roberts, and B. Yoshida, Chaos in quantum channels, *Journal of High Energy Physics* **2016**, 4 (2016).
- [65] E. Iyoda and T. Sagawa, Scrambling of quantum information in quantum many-body systems, *Phys. Rev. A* **97**, 042330 (2018).
- [66] A. Seshadri, V. Madhok, and A. Lakshminarayan, Tripartite mutual information, entanglement, and scrambling in permutation symmetric systems with an application to quantum chaos, *Phys. Rev. E* **98**, 052205 (2018).
- [67] P. Hayden, M. Headrick, and A. Maloney, Holographic mutual information is monogamous, *Phys. Rev. D* **87**, 046003 (2013).
- [68] M. Rota, Tripartite information of highly entangled states, *Journal of high energy physics* **2016**, 75 (2016).
- [69] M. Asadi and M. Ali-Akbari, Holographic mutual and tripartite information in a symmetry breaking quench, *Physics Letters B* **785**, 409 (2018).
- [70] M. Ali-Akbari, M. Rahimi, and M. Asadi, Holographic mutual and tripartite information in a non-conformal background, *Nuclear Physics B* **964**, 115329 (2021).
- [71] O. Schnaack, N. Bölter, S. Paeckel, S. R. Manmana, S. Kehrein, and M. Schmitt, Tripartite information, scrambling, and the role of Hilbert space partitioning in quantum lattice models, *Phys. Rev. B* **100**, 224302 (2019).
- [72] L. Nie, M. Nozaki, S. Ryu, and M. T. Tan, Signature of quantum chaos in operator entanglement in 2d CFTs, *Journal of Statistical Mechanics: Theory and Experiment* **2019**, 093107 (2019).
- [73] K. A. Landsman, C. Figgatt, T. Schuster, N. M. Linke, B. Yoshida, N. Y. Yao, and C. Monroe, Verified quantum information scrambling, *Nature* **567**, 61 (2019).
- [74] M. S. Blok, V. V. Ramasesh, T. Schuster, K. O'Brien, J. M. Kreikebaum, D. Dahlen, A. Morvan, B. Yoshida, N. Y. Yao, and I. Siddiqi, Quantum Information Scrambling on a Superconducting Qutrit Processor, *Phys. Rev. X* **11**, 021010 (2021).
- [75] J. Kudler-Flam, R. Sohal, and L. Nie, Information Scrambling with Conservation Laws, *SciPost Phys.* **12**, 117 (2022).
- [76] Q. Zhu, Z.-H. Sun, M. Gong, F. Chen, Y.-R. Zhang, Y. Wu, Y. Ye, C. Zha, S. Li, S. Guo, H. Qian, H.-L. Huang, J. Yu, H. Deng, H. Rong, J. Lin, Y. Xu, L. Sun, C. Guo, N. Li, F. Liang, C.-Z. Peng, H. Fan, X. Zhu, and J.-W. Pan, Observation of Thermalization and Information Scrambling in a Superconducting Quantum Processor, *Phys. Rev. Lett.* **128**, 160502 (2022).
- [77] H. P. Breuer and F. Petruccione, *The theory of open quantum systems* (Oxford University Press, 2002).
- [78] C. Gardiner and P. Zoller, *Quantum noise: a handbook of Markovian and non-Markovian quantum stochastic methods with applications to quantum optics* (Springer Science & Business Media, 2004).
- [79] A. Barchielli and M. Gregoratti, *Quantum trajectories and measurements in continuous time: the diffusive case*, Vol. 782 (Springer, 2009).
- [80] I. Peschel and V. Eisler, Reduced density matrices and entanglement entropy in free lattice models, *Journal of Physics A: Mathematical and Theoretical* **42**, 504003 (2009).
- [81] A. Polkovnikov, K. Sengupta, A. Silva, and M. Vengalattore, Colloquium: Nonequilibrium dynamics of closed interacting quantum systems, *Rev. Mod. Phys.* **83**, 863 (2011).
- [82] J.-S. Caux and F. H. L. Essler, Time Evolution of Local Observables After Quenching to an Integrable Model, *Phys. Rev. Lett.* **110**, 257203 (2013).
- [83] J.-S. Caux, The Quench Action, *Journal of Statistical Mechanics: Theory and Experiment* **2016**, 064006 (2016).
- [84] P. Calabrese, F. H. L. Essler, and G. Mussardo, Introduction to ‘Quantum Integrability in Out of Equilibrium Systems’, *Journal of Statistical Mechanics: Theory and Experiment* **2016**, 064001 (2016).
- [85] F. H. L. Essler and M. Fagotti, Quench dynamics and relaxation in isolated integrable quantum spin chains, *Journal of Statistical Mechanics: Theory and Experiment* **2016**, 064002 (2016).
- [86] L. Vidmar and M. Rigol, Generalized Gibbs ensemble in integrable lattice models, *Journal of Statistical Mechanics: Theory and Experiment* **2016**, 064007 (2016).
- [87] See Supplemental Material for details.
- [88] A. Peres, Separability Criterion for Density Matrices, *Phys. Rev. Lett.* **77**, 1413 (1996).
- [89] K. Życzkowski, P. Horodecki, A. Sanpera, and M. Lewenstein, Volume of the set of separable states, *Phys. Rev. A* **58**, 883 (1998).
- [90] J. Eisert and M. B. Plenio, A comparison of entanglement measures, *Journal of Modern Optics* **46**, 145 (1999).
- [91] G. Vidal and R. F. Werner, Computable measure of entanglement, *Phys. Rev. A* **65**, 032314 (2002).
- [92] H. Shapourian, K. Shiozaki, and S. Ryu, Partial time-reversal transformation and entanglement negativity in fermionic systems, *Phys. Rev. B* **95**, 165101 (2017).
- [93] H. Shapourian and S. Ryu, Finite-temperature entanglement negativity of free fermions, *Journal of Statistical Mechanics: Theory and Experiment* **2019**, 043106 (2019).
- [94] H. Shapourian, P. Ruggiero, S. Ryu, and P. Calabrese, Twisted and untwisted negativity spectrum of free fermions, *SciPost Phys.* **7**, 37 (2019).
- [95] M. Gruber and V. Eisler, Time evolution of entanglement negativity across a defect, *Journal of Physics A: Mathematical and Theoretical* **53**, 205301 (2020).
- [96] P. Calabrese, J. Cardy, and E. Tonni, Entanglement negativity in extended systems: a field theoretical approach, *Journal of Statistical Mechanics: Theory and Experiment* **2013**, P02008 (2013).
- [97] A. Coser, E. Tonni, and P. Calabrese, Entanglement negativity after a global quantum quench, *Journal of Statistical Mechanics: Theory and Experiment* **2014**, P12017 (2014).
- [98] V. Alba and P. Calabrese, Quantum information dynamics in multipartite integrable systems, *EPL (Europhysics Letters)* **126**, 60001 (2019).
- [99] B. Bertini, E. Tartaglia, and P. Calabrese, Entanglement

and diagonal entropies after a quench with no pair struc-

ture, *Journal of Statistical Mechanics: Theory and Experiment* **2018**, 063104 (2018).

SUPPLEMENTAL MATERIAL

Entangled multiplets and unusual spreading of quantum correlations in a continuously monitored tight-binding chain

Federico Carollo¹ and Vincenzo Alba²

¹*Institut für Theoretische Physik, Universität Tübingen,
Auf der Morgenstelle 14, 72076 Tübingen, Germany*

²*Dipartimento di Fisica, Università di Pisa, and INFN Sezione di Pisa, Largo Bruno Pontecorvo 3, Pisa, Italy*

I. PREDICTION FROM THE COLLAPSED QUASIPARTICLE ANSATZ

From the collapsed quasiparticle ansatz—which is a stochastic theory—it is possible to obtain predictions for average quantities. Here, we show how to do this for entanglement-related quantities. In the first subsection, we discuss the case of a single subsystem. This result was derived in Ref. [4] and we review it here also to clarify the scaling limit in which the theory should be expected to be valid. In the second subsection, we instead provide a new prediction, within the collapsed quasiparticle ansatz, for the mutual information and the logarithmic negativity between two subsystems embedded in an infinite chain.

A. The case of a single subsystem

For a single subsystem of length ℓ and in the absence of continuous monitoring, the dynamics of the entanglement entropies is described by the following formula [58, 60, 61]

$$S_\ell^{(n),0}(t) \approx \int_{-\pi}^{\pi} \frac{dq}{2\pi} s_q^{(n)} \min \{2|v_q|t, \ell\} . \quad (\text{S1})$$

The above relation provides the leading-order behavior in ℓ of the entropy and is valid for large times. This can be made explicit by introducing the scaling limit $\ell \rightarrow \infty$, with $t/\ell = \tau$ fixed. In this limit, we have

$$\mathbf{s}^{(n),0}(\tau) := \lim_{\ell \rightarrow \infty} \frac{S_\ell^{(n),0}(\tau\ell)}{\ell} = \int_{-\pi}^{\pi} \frac{dq}{2\pi} s_q^{(n)} \min \{2|v_q|\tau, 1\} , \quad (\text{S2})$$

which is also the prediction used in the main text for the unitary quasiparticle picture.

In Ref. [4], it was suggested that, in the presence of continuous monitoring, the entanglement entropies, averaged over all possible realizations of the stochastic process, obey the following relation

$$\overline{S}_\ell^{(n)}(t) = \mathbb{E} \left[S_\ell^{(n)}(t) \right] \approx e^{-\gamma t} \int_{-\pi}^{\pi} \frac{dq}{2\pi} s_q^{(n)} \min \{2|v_q|t, \ell\} + \gamma \int_0^t du e^{-\gamma u} \int_{-\pi}^{\pi} \frac{dq}{2\pi} s_q^{(n)} \min \{2|v_q|u, \ell\} . \quad (\text{S3})$$

The above formula is specialized for the case of a (macroscopically) homogeneous initial state, such as the one considered in the main text. A straightforward calculation leads to the following simplified expression

$$\overline{S}_\ell^{(n)}(t) \approx \int_{-\pi}^{\pi} \frac{dq}{2\pi} \frac{2|v_q|}{\gamma} \left(1 - e^{-\gamma \min \{t, \frac{\ell}{2|v_q|}\}} \right) s_q^{(n)} . \quad (\text{S4})$$

It is important to look at this formula in the scaling limit. This is indeed essential to systematically compare the prediction from the theory with numerical simulations and to establish the validity of the theory.

The definition of a proper limit for the above formula requires a bit of care. Indeed, one should note that, in the scaling limit in which the quasiparticle picture becomes well-defined, time diverges as $t = \tau\ell \rightarrow \infty$. As such, the exponential function would converge to 0 as soon as $\tau > 0$, unless a proper rescaling of γ is introduced. This is also shown by numerical results presented in Fig. S1(a). Clearly, by looking at the arguments of the min function, the correct scaling of γ is $\gamma = \Gamma/\ell$, with Γ independent on ℓ . Finally, due to the appearance of a factor γ^{-1} in the integral, a well-defined limit is obtained by dividing $\overline{S}_\ell^{(n)}(t)$ by ℓ . Note that this scaling limit is the most natural one, emerging when considering hydrodynamic theories in combination with dissipative effects. It was also recognized in Ref. [4] but

it is actually the same, in spirit, dissipative limit considered, e.g., in Refs. [44, 48], where time is taken in units of the (small) dissipative rate, i.e. γt is kept fixed.

Collecting these observations, we define the scaling limit $\ell \rightarrow \infty$, with $t/\ell = \tau$ and $\gamma t = \Gamma\tau$ fixed. In this limit, we find

$$\mathbf{s}^{(n)}(\tau) = \lim_{\ell \rightarrow \infty} \frac{\overline{S}_\ell^{(n)}(t)}{\ell} = \int_{-\pi}^{\pi} \frac{dq}{2\pi} \frac{2|v_q|}{\Gamma} \left(1 - e^{-\Gamma \min\{\tau, \frac{1}{2|v_q|}\}} \right) s_q^{(n)}, \quad (\text{S5})$$

which is the scaling function predicted by the collapsed quasiparticle ansatz and plotted in Fig. 2(a-b). We note that, for our initial state we have $s_q^{(n)} = \log 2$ for all n , and the same quantitative prediction holds for all entanglement entropies.

B. The case of two (adjacent) subsystems

We now focus on the prediction, derived from the assumptions of the collapsed quasiparticle ansatz, for quantum correlations and entanglement between two adjacent subsystems of length ℓ .

We start considering the mutual information between these subsystems. As for the previous case, the starting point is the prediction for the unitary case, given by

$$I_2^0(t) \approx \int_{-\pi}^{\pi} \frac{dq}{2\pi} \Theta_q(t) \log 2, \quad (\text{S6})$$

where the factor $\log 2$ comes from considering the correlation content of quasiparticles which is given by the von Neumann Yang-Yang entropy. The function $\Theta_q(t)$ is here given by

$$\Theta_q(t) = 2|v_q|t + 2 \max\{|v_q|t, \ell\} - 2 \max\{2|v_q|t, \ell\}. \quad (\text{S7})$$

With the above formula, we can directly write down the prediction from the collapsed quasiparticle ansatz. In the same spirit of Eq. (S3), we have

$$\overline{I}_2(t) = \mathbb{E}[I_2(t)] \approx e^{-\gamma t} \int_{-\pi}^{\pi} \frac{dq}{2\pi} \Theta_q(t) \log 2 + \gamma \int_0^t du e^{-\gamma u} \int_{-\pi}^{\pi} \frac{dq}{2\pi} \Theta_q(u) \log 2. \quad (\text{S8})$$

A lengthy but straightforward calculation gives

$$\overline{I}_2(t) \approx \log 2 \int_{-\pi}^{\pi} \frac{dq}{2\pi} \left[e^{-\gamma t} \Theta_q(t) + J_1 \left(\min \left\{ t, \frac{\ell}{2|v_q|} \right\} \right) + J_2 \left(\min \left\{ t, \frac{\ell}{|v_q|} \right\}, \min \left\{ t, \frac{\ell}{2|v_q|} \right\} \right) \right], \quad (\text{S9})$$

where we have

$$J_1(t) = \gamma \int_0^t du e^{-\gamma u} 2|v_q|u \quad \text{and} \quad J_2(t, s) = \gamma \int_s^t du e^{-\gamma u} [2\ell - 2|v_q|u].$$

When properly considering the scaling limit discussed in the previous section, the prediction becomes

$$\lim_{\ell \rightarrow \infty} \frac{\overline{I}_2(\tau\ell)}{\ell} = \log 2 \int_{-\pi}^{\pi} \frac{dq}{2\pi} \left[e^{-\Gamma\tau} \Theta_q(t) + j_1 \left(\min \left\{ \tau, \frac{1}{2|v_q|} \right\} \right) + j_2 \left(\min \left\{ \tau, \frac{1}{|v_q|} \right\}, \min \left\{ \tau, \frac{1}{2|v_q|} \right\} \right) \right], \quad (\text{S10})$$

with the rescaled integrals

$$j_1(\tau) = \Gamma \int_0^\tau du e^{-\Gamma u} 2|v_q|u, \quad \text{and} \quad j_2(\tau, \sigma) = \Gamma \int_\sigma^\tau du e^{-\Gamma u} [2 - 2|v_q|u].$$

The formula in Eq. (S10) is the one plotted in Fig. 2(c) for the collapsed quasiparticle ansatz. Furthermore, from the above formula we can also find the stationary value for the mutual information. This can be found by taking the limit $\tau \rightarrow \infty$, which gives

$$\lim_{\tau \rightarrow \infty} \lim_{\ell \rightarrow \infty} \frac{\overline{I}_2(\tau\ell)}{\ell} = \frac{\log 2}{\Gamma} \int_{-\pi}^{\pi} \frac{dq}{\pi} \left(1 - e^{-\Gamma/(2|v_q|)} \right)^2 |v_q|. \quad (\text{S11})$$

We now briefly comment on the prediction for the logarithmic negativity between the two adjacent intervals. We first observe that the logarithmic negativity for the unitary case, \mathcal{E}_2^0 , has been shown to be equivalent to half of the mutual information, i.e., $\mathcal{E}_2^0 = I_2^0/2$, since in our case the latter is equal to the Rényi-1/2 mutual information. Because of this, the prediction for the logarithmic negativity in the continuously monitored system is immediately found as $\overline{\mathcal{E}}_2 = \overline{I}_2/2$.

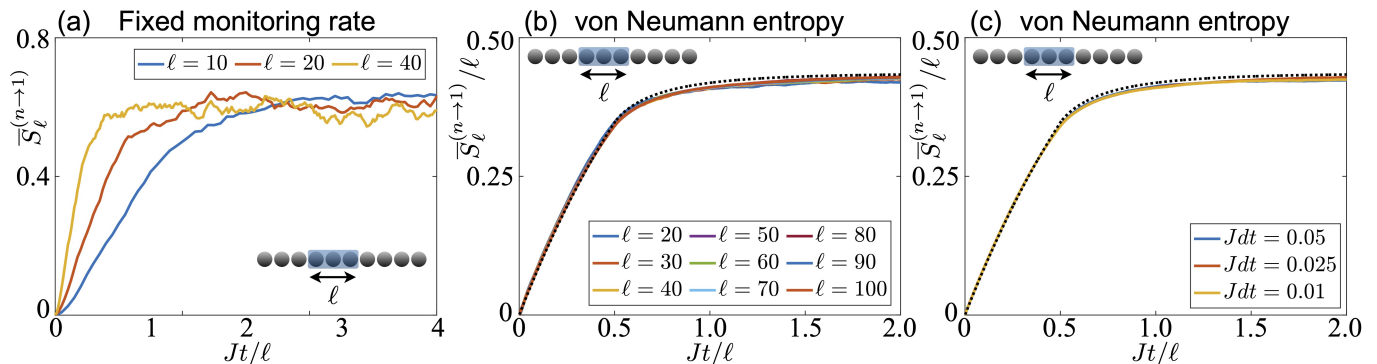


FIG. S1. **Additional results.** (a) Plot of the von Neumann entanglement entropy for a subsystem of length ℓ embedded in the many-body chain. The plot is done in the scaling limit in which the unitary quasiparticle picture is expected to emerge. Note however that we are not dividing the entropy by ℓ . In this case, we consider a fixed $\gamma = J$. The curves we display, for $\ell = 10, 20, 40$, show that in this case there is no scaling behavior. The entropy is averaged over $N_{\text{traj}} = 200$ trajectories. (b) Comparison of numerical results for the von Neumann entanglement entropy (in the scaling limit $t, \ell \rightarrow \infty$ with $t/\ell = \tau$ fixed and $\gamma\ell = \Gamma$ fixed) and the prediction from the collapsed quasiparticle ansatz (dotted line). Here, we set $\Gamma = 1$. While the prediction is closer to the numerical results than what we observed for the other entropies shown in the main text, it seems that a perfect agreement is not reached. The entropy is averaged over $N_{\text{traj}} = 250$ and here we considered $Jdt = 0.025$. (c) Plot of the von Neumann entanglement entropy in the scaling regime, for different values of Jdt . As shown, for the considered values of Jdt , it is not possible to appreciate relevant changes in the behavior of the von Neumann entropy. We consider $N_{\text{traj}} = 50$ for $Jdt = 0.05$, $N_{\text{traj}} = 200$ for $Jdt = 0.025$ and $N_{\text{traj}} = 100$ for $Jdt = 0.01$.

II. DETAILS ON THE NUMERICAL SIMULATIONS

The numerical simulations of quantum trajectories were performed using the method discussed in Refs. [4, 8]. The curves plotted in Fig. 2 and in Fig. 3(d) have been obtained by simulating a system with $L = 1000$ sites and ℓ up to $\ell = 100$. We have discretized time using a time step $Jdt = 0.025$ and we have verified that our results are not substantially changed by considering a larger $Jdt = 0.05$ nor a smaller one, $Jdt = 0.01$ [see e.g. Fig. (S1)(c)]. The curves are obtained by taking the average over a different number of quantum trajectories of the stochastic process [see caption of Fig. 2 and Fig. 3]. The plots in Fig. 3(a-b-c) are for $\gamma \equiv 0$. These curves do not require averaging over trajectories since the dynamics is deterministic and are also free of time-discretization (Trotter) errors.

III. ADDITIONAL RESULTS

In this section, we make two important considerations. First, we show that if γ is not rescaled as $\gamma = \Gamma/\ell$ then the entanglement entropies do not show scaling behavior when considering the limit $t, \ell \rightarrow \infty$ with t/ℓ fixed. This can be observed in Fig. S1(a), where we plot the entanglement entropy $S_\ell^{(n \rightarrow 1)}$ as a function of Jt/ℓ . As shown, increasing ℓ the entanglement entropy tends to converge faster and faster to its stationary behavior and, thus, it cannot show a proper scaling behavior. This, in addition to the discussion in the main text, shows that in order to arrive at a proper scaling limit, γ needs to be rescaled in a way that γt is also fixed in the limit.

We further show numerical results, in the appropriate scaling limit discussed in the main text and in this supplemental material, for the von Neumann entanglement entropy investigated in Ref. [4]. We can observe that, also in this case, the numerical results seem not to converge to the prediction from the collapsed quasiparticle ansatz, even if, in this case, the prediction is much more accurate. This is shown in Fig. S1(b). In Fig. (S1)(c), we show that the discrepancy found in Fig. (S1)(b), between numerical results and collapsed quasiparticle ansatz, does not seem to be related to a time-discretization Trotter error.

IV. VANISHING OF TRIPARTITE INFORMATION WITH TRIPLET

In this section we consider the state $\prod_{j=0}^{L/\nu-1} a_{\nu j+1}^\dagger |0\rangle = |10\dots 0100100\dots\rangle$. For $\nu = 3$, this state is a source of triplets of quasiparticles for the considered Hamiltonian and here we show that, in this case, the tripartite information I_3 vanishes in the scaling limit.

For the above state, ν species of quasiparticles exist. They have group velocities v_p^j

$$v_p^j = J \sin \left(p - \frac{2(j-1)\pi}{\nu} \right), \quad \text{with } j = 1, 2, \dots, \nu. \quad (\text{S12})$$

Here j labels the different species of quasiparticles. The quasimomentum k_p^j of the quasiparticles is

$$k_p^j = p - \frac{2(j-1)\pi}{\nu}, \quad (\text{S13})$$

where

$$p \in \left[\pi - \frac{2\pi}{\nu}, \pi \right]. \quad (\text{S14})$$

For $\nu = 2$ one recovers the standard case of entangled pairs of quasiparticles. Now the two species of quasiparticles have $p \in [0, \pi]$ and quasimomenta $k_p^1 \in [0, \pi]$, whereas $k_p^2 \in [-\pi, 0]$. This means that $v_p^1 = -v_p^2$.

Now for the case with $\nu = 3$ one has different possible orderings for the quasiparticles velocities as

$$v_p^2 < v_p^3 < 0, v_p^1 > 0 \quad \frac{\pi}{3} \leq p < \frac{\pi}{2} \quad (\text{S15})$$

$$v_p^3 < v_p^2 < 0, v_p^1 > 0 \quad \frac{\pi}{2} \leq p < \frac{2\pi}{3} \quad (\text{S16})$$

$$v_p^3 < 0, v_p^2 > 0, v_p^2 < v_p^1 \quad \frac{2\pi}{3} \leq p < \frac{5\pi}{6} \quad (\text{S17})$$

$$v_p^3 < 0, v_p^1 > 0, v_p^2 > v_p^1 \quad \frac{5\pi}{6} \leq p < \pi \quad (\text{S18})$$

This means that the triplets of quasiparticles for a generic label p can be arranged as in Fig. S2.

Let us now discuss the contribution of the triplets to the entanglement entropy. Crucially, this depends in the specific way in which the entangled quasiparticles are shared. Let us consider two subsystems X and Y . The contribution of a ν -plet of entangled quasiparticles to the entanglement entropy between them is denoted as $s_p^{\{j_i\}}$. Here $j_i = 1, 2, \dots, \nu$ and $i = 0, 1, \dots, m$ with m being the number of quasiparticles in X . It has been postulated in Ref. [99] that

$$s_p^{\{j_i\}} = - \left(\sum_{i=1}^m \varrho_p^{(j_i)} \right) \ln \left(\sum_{i=1}^m \varrho_p^{(j_i)} \right) - \left(1 - \sum_{i=1}^m \varrho_p^{(j_i)} \right) \ln \left(1 - \sum_{i=1}^m \varrho_p^{(j_i)} \right). \quad (\text{S19})$$

Here the densities $\varrho_p^{(j_i)}$ are defined as

$$\varrho_p^{(j)} = \varrho \left(p - \frac{2(j-1)\pi}{\nu} \right), \quad (\text{S20})$$

where $\varrho(k)$ is the density describing the stationary value of local observables, and it is calculated as

$$\varrho(k) = \langle \psi(0) | \beta_k^\dagger \beta_k | \psi(0) \rangle. \quad (\text{S21})$$

Importantly, one has that the entropy contribution satisfies

$$s_p^{\{j_i\}} = s_p^{\{j_i\}_c}, \quad \text{with } \{j_i\}_c = \{1, 2, \dots, \nu\} / \{j_i\}. \quad (\text{S22})$$

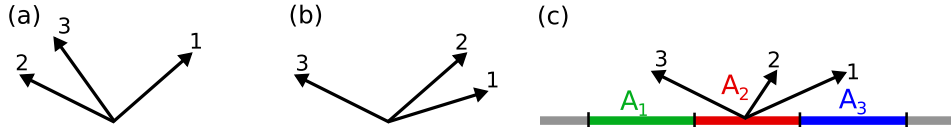


FIG. S2. **Entangling triplets.** We show two possible quasiparticles configurations. In (a) quasiparticles 2, 3 have negative velocities, whereas quasiparticle 1 has positive one. This corresponds to $\pi/3 \leq p \leq \pi/2$. In (b) quasiparticles 1, 2 have positive velocities, and 3 has a negative one. This corresponds to $2/3\pi \leq p \leq 5/6\pi$. Two other equivalent configurations are obtained by exchanging $2 \leftrightarrow 3$ in (a) and $1 \leftrightarrow 2$ in (b), which give $\pi/2 \leq p \leq 2/3\pi$ and $5/6\pi \leq p \leq \pi$, respectively. (c) Configuration with quasiparticles of a same triplet shared by three subsystems, A_1, A_2 and A_3 .

This means that $s_p^{\{j_i\}}$ is symmetric under exchange of the particles that are in and out of a subsystem. This property ensures that the entanglement entropy of two complementary subsystems is the same, i.e., $S_X = S_Y$ if $Y = \bar{X}$. As we show, this also implies a vanishing tripartite information if only entangled triplets are present.

For the case of triplets we have the contributions

$$s_p^{\{1\}} = s_p^{\{2,3\}} \quad (\text{S23})$$

$$s_p^{\{2\}} = s_p^{\{1,3\}} \quad (\text{S24})$$

$$s_p^{\{3\}} = s_p^{\{1,2\}}. \quad (\text{S25})$$

The only arrangement of quasiparticles for which one might expect a non-zero tripartite mutual information is that with the triplet shared by the three subsystems. This is a configuration like the one shown in Fig. S2 (c). System A is tripartite as $A = A_1 \cup A_2 \cup A_3$. In the configuration we have that A_1 contains a quasiparticle of species 3, A_2 one of species 2, and A_3 of species 1. Notice that although there could be entangled multiplets shared between the subsystems and the remainder of A , we can neglect them because they cancel when constructing the mutual information. Let us consider the tripartite mutual information

$$I_3 = I_2[A_2, A_1] + I_2[A_2, A_3] - I_2[A_2, A_1 \cup A_3]. \quad (\text{S26})$$

Now it is clear that

$$I_2[A_2, A_1] = s_p^{\{2\}} + s_p^{\{3\}} - s_p^{\{2,3\}} \quad (\text{S27})$$

$$I_2[A_2, A_3] = s_p^{\{2\}} + s_p^{\{1\}} - s_p^{\{1,2\}} \quad (\text{S28})$$

$$I_2[A_2, A_1 \cup A_3] = s_p^{\{2\}} + s_p^{\{1,3\}}, \quad (\text{S29})$$

where in the last row we used that $s^{\{1,2,3\}} = 0$. Now, after substituting Eqs. (S27)-(S28)-(S29) in Eq. (S26), by using Eqs. (S23)-(S24)-(S25), we find that I_3 vanishes. This argument can be adapted to any triplet arrangement.